Journal of the Optical Society of America B
OPTICAL PHYSICS

# Extracting correlation length in Mott insulators by strong-field driving

Abdallah AlShafey,[1,*] Xu-Yan Jia,[2] Yuan-Ming Lu,[1] Shou-Shu Gong,[3,4] Gerard McCaul,[5] Denys Bondar,[5] Mohit Randeria,[1] Takashi Oka,[6] and Alexandra S. Landsman[1,7]

[1]Department of Physics, The Ohio State University, Columbus, Ohio 43210, USA
[2]Department of Physics, Beihang University, Beijing 100191, China
[3]School of Physical Sciences, Great Bay University, Dongguan 523000, China
[4]Great Bay Institute for Advanced Study, Dongguan 523000, China
[5]Tulane University, New Orleans, Louisiana 70118, USA
[6]The Institute for Solid State Physics, The University of Tokyo, Kashiwa, Chiba 277-8581, Japan
[7]landsman.7@osu.edu
*alshafey.1@osu.edu

Received 12 December 2023; revised 24 March 2024; accepted 27 March 2024; posted 2 April 2024; published 22 April 2024

**The breakdown of a Mott-insulator when subjected to intense laser fields is characterized by the formation of doublon-hole pairs. This breakdown is furthermore evidenced by the production of high harmonics that can be experimentally measured. Here, we present an approach for extracting the doublon-hole correlation length of a Mott insulator. The method is based on a dynamical calculation of the Mott insulator's rate of charge production in response to an applied strong-field laser pulse. We find that coupling the Mott insulator to a metal drastically increases the correlation length, in support of our recent hypothesis [Phys. Rev. B 108, 144434 (2023)] that coupling to a metal enhances the charge fluctuations in the insulator. We confirm our conclusions using density matrix renormalization group (DMRG) calculations. The proposed method can be applied to experimentally measured observables, such as differential reflectivity or the high harmonic generation (HHG) spectrum to extract doublon-hole correlation length.** © 2024 Optica Publishing Group

https://doi.org/10.1364/JOSAB.515940

## 1. INTRODUCTION

Since the advent of the laser and its subsequent application to probe states of matter, the theoretical study of strong-field physics has quickly gained momentum. The framework developed by Keldysh [1] is generally accepted as the basic model describing the ionization of atoms and solid media under the influence of strong electromagnetic fields with frequencies lower than the ionization potential [2–5]. Keldysh realized that strong-field ionization can be understood as a consequence of either quantum tunneling or multiphoton absorption depending on the laser and material parameters. The quantum tunneling regime, which is dominant in the DC limit and is the relevant regime in this study, is characterized by a threshold field, which must be exceeded in order for ionization to occur. More recently, there has been growing interest in the strong-field physics of correlated quantum materials, with specific focus on Mott insulators [6–13]. When driven with a strong-field pulse, a macroscopic number of elementary charge excitations known as doublons and holes is produced within the insulator [14–21]. The energy required to produce a doublon-hole pair and the Mott gap $\Delta_{\mathrm{Mott}}$, along with their correlation length $\xi$, is central to the strong-field physics involved since it determines the threshold field required for efficient quantum tunneling,

$$F_{\mathrm{th}} = \Delta_{\mathrm{Mott}}/2\xi, \tag{1}$$

and therefore dictates the field strength beyond which a breakdown of the insulating state occurs.

Recently, we investigated the effect of coupling a Mott insulator to a metal on the doublon production and produced high-order harmonics at the interface [22]. We found that an increased interfacial coupling enhances high harmonic production inside the insulator and suggested an increased doublon-hole correlation length as the reason behind this lowered threshold for response. In the present paper, we aim to verify this claim. We outline a method for extracting the doublon-hole correlation length $\xi$ in Mott insulators that are coupled to a free conducting chain in a metal/insulator interface. The method closely follows that of Oka [14] and relates the *static* parameters $\xi$ and $\Delta_{\mathrm{Mott}}$ to the *dynamical* rate of charge production $\Gamma$ in response to a strong-field pulse. Moreover, since $\Gamma$ was shown to be directly related to the differential reflectivity $\Delta R/R$ [23], an experimental quantity, the method provides

a way of accessing $\xi$ experimentally. We find that an increased interfacial coupling between metal and insulator does in fact lead to an increased correlation length in the insulator, supporting our hypothesis. The result is further tested by comparison with independent *static* DMRG calculations.

## 2. PROPERTIES OF THE UNCOUPLED MOTT INSULATOR

A popular model exhibiting the Mott insulating phase is the half-filled one-dimensional Hubbard chain:

$$H = -t_0 \sum_{i,\sigma}^{L} \left( c^{\dagger}_{i+1,\sigma} c_{i,\sigma} + \text{h.c.} \right) + U \sum_{i,\sigma}^{L} \left( n_{i,\uparrow} - \frac{1}{2} \right) \left( n_{i,\downarrow} - \frac{1}{2} \right). \tag{2}$$

The model has a known analytic solution given by the Bethe ansatz [24–26]. Charge excitations in this model constitute doubly occupied sites (doublons) and empty sites (holes). Additionally, charge conservation in the model necessitates that doublons and holes are created in pairs. These doublon-hole pairs are the elementary charge excitations in the Hubbard model and are the central focus of our study.

In the $U = 0$ limit the electrons are fully delocalized and, in the ground state, occupy the lower half of a dispersing band $\epsilon(k) = -2t_0 \cos k$, forming a band metal. Since this limit does not energetically distinguish between the four possible states $(|\cdot\rangle, |\uparrow\rangle, |\downarrow\rangle, |\uparrow\downarrow\rangle)$ on a given site, the ground state average doublon density is a quarter ($D_{\text{g.s.}} = 1/4$). The charge gap in this limit is zero, and the correlation length diverges. The opposite limit $t_0 = 0$ results in the extreme localization of electrons; no electron is allowed to hop from site to site. The ground state is then a product of singly occupied sites, since double occupancy requires an energy cost on the order of $U$, while the correlation length becomes very small. For a small finite $t_0 \ll U$, a second-order perturbative correction adds an effective antiferromagnetic exchange $J_{\text{eff}} = 4t_0^2/U$ between nearest-neighbor sites. This can be understood intuitively on the basis of Pauli's exclusion principle. The nonzero hopping $t_0$ favors electron delocalization via virtual states of neighboring doublons and holes. These virtual hopping processes would be blocked in the case of parallel neighboring spins; thus, antiferromagnetism is favored. In the intermediate regime, the average doublon density will be $0 < D_{\text{g.s.}} < 1/4$. Thus,

$$D_{\text{g.s.}} \equiv \frac{1}{L} \sum_{i}^{L} \langle \psi_{\text{g.s.}} | n_{i,\uparrow} n_{i,\downarrow} | \psi_{\text{g.s.}} \rangle \to 0 \quad (t_0/U \ll 1) \to 1/4 \quad (t_0/U \gg 1). \tag{3}$$

Applying a large electric field to the Mott insulator can result in dielectric breakdown, during which doublon-hole pairs are produced, marking an increase in $D_{\text{g.s.}}$. It is therefore useful to track $D_{\text{g.s.}}(t)$ as a measure of dielectric breakdown as a driving field is applied.

Finally, we note the analytical expressions for the Mott gap $\Delta_{\text{Mott}}$ and the correlation length $\xi$ as functions of $U/t_0$ within the Hubbard model:

$$\Delta_{\text{Mott}}/t_0 = -2 + \frac{U}{2t_0} + 2 \int_0^{\infty} \frac{d\omega}{\omega} \frac{J_1(\omega) e^{-\frac{U\omega}{4t_0}}}{\cosh \frac{U\omega}{4t_0}},$$

$$(\xi/a)^{-1} = \frac{4t_0}{U} \int_1^{\infty} \mathrm{d}y \frac{\ln\left(y + \sqrt{y^2 - 1}\right)}{\cosh \frac{2\pi t_0 y}{U}}. \tag{4}$$

The quantities are plotted later in Fig. 2(a).

## 3. DRIVING A METAL-INSULATOR INTERFACE

The model under consideration [Figs. 1(a) and 1(b)] couples the one-dimensional Mott insulator to a metallic chain and to a driving field $F(t) = -\partial A/\partial t$, where

$$A(t) = \frac{F_0}{\omega_0} \sin^2 \left( \frac{\omega_0 t}{2N} \right) \sin(\omega_0 t), \tag{5}$$

where $F_0$ is the maximum field amplitude and $\omega_0$ is the central frequency. The Hamiltonian is

$$H = -t_0 \sum_{i,\sigma,\alpha}^{L} e^{-i\phi(t)} c^{\dagger}_{i+1,\sigma,\alpha} c_{i,\sigma,\alpha} + \text{h.c.} - g \sum_{i,\sigma}^{L} e^{-i\phi(t)} c^{\dagger}_{i,\sigma,A} c_{i,\sigma,B} + \text{h.c.} + U \sum_{i,\sigma}^{L} (n_{i,\uparrow,A} - 1/2)(n_{i,\downarrow,A} - 1/2), \tag{6}$$

where the coupling to the field is introduced by the Peierls substitution $t_0 \to t_0 e^{-i\phi(t)}$, with $\phi(t) = aA(t)$ and $a$ being the lattice constant. Here we use $a = 4$ Å and $t_0 = 0.52$ eV to mimic the 1D Mott insulator $Sr_2CuO_3$ [14,15]. $g$ is the tunable interfacial coupling, and $U$ is the tunable Hubbard repulsion. Equation (6) with $\phi = 0$ was used in [28] to model $PdCrO_2$, a magnetic oxide metal displaying Kondo lattice physics.

Let us first discuss the $g = 0$ limit. The response in this limit depends on the dimensionless Keldysh parameter $\gamma_K \equiv \hbar\omega_0/\xi F_0$ and has been studied in [14]. In the tunneling regime, $\gamma_K \ll 1$, the dominant process exciting the charge gap is the electric field $F_0$ pulling apart doublon-hole pairs and polarizing and breaking down the insulating state. This mechanism is reminiscent of the Schwinger mechanism in vacuum [29], where an electric field large enough ($F_0^{\text{vac}} \gtrsim 10^{18}$ V/m) will polarize the vacuum, excite the charge gap $\Delta_{\text{vac}} = 2m_e c^2$, and create electron-positron pairs on a much lower energy scale. The rate of pair production becomes exponentially sensitive to the field strength, $\Gamma \propto \exp\{-\pi \frac{F_{\text{th}}}{F_0}\}$, exhibiting a threshold behavior. Here $F_{\text{th}} = \Delta_{\text{Mott}}/2\xi$, explaining the central role both quantities play in strong-field physics. Noting that $\Delta_{\text{Mott}}$ increases and $\xi$ decreases monotonically (see Fig. 2) with $U$, we see that breakdown of the insulating state is possible for small $U$ but will fail for larger $U$ as soon as $F_0 < F_{\text{th}}$. For a field

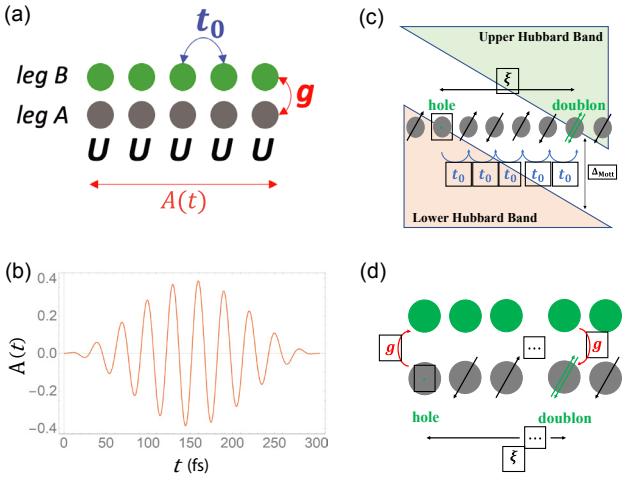


**Fig. 1.** (a) Model of the coupled metal/Mott-insulator system. (b) Vector potential $A(t)$ as a function of time. (c) In the uncoupled one-dimensional Mott insulator, $N$ hoppings $t_0$ are required to create a pair of size $\xi = Na$. (d) In the coupled system, a doublon-hole pair of arbitrary size can be created by just two hoppings $g$ as illustrated.

strength $F_0 = 10^9$ V/m, the insulating state is preserved for values $U > U_{\text{th}} \sim 6t_0$ [15].

Here, we are always in the tunneling regime with $\gamma_K \ll 1$, where the rate of doublon-hole pair production is

$$\Gamma_{\text{tunnel}} \propto \exp - \left\{ \frac{\pi}{2} \frac{\Delta_{\text{Mott}}}{\xi F_0} \right\}. \tag{7}$$

Electrons must tunnel through a tilted barrier [Fig. 1(c)] to create the doublon-hole pair [14]. As we start coupling the insulator to a metal ($g \neq 0$), entirely new mechanisms of producing the charge excitations emerge [Fig. 1(d)]. The metal leg can now donate an electron on one site while removing an electron from another distant site through just *two* interfacial hoppings $g$. This is expected to considerably increase the correlation length $\xi$ from the uncoupled insulator limit $g = 0$.

To calculate this increase in $\xi$ we drive the interface with tunable intensity $10^9$ V/m $\leq F_0 \leq 3 \times 10^9$ V/m and central frequency $\omega_0 = 32.9$ THz. The whole range of intensities is above $F_{\text{th}}$ as evidenced by a finite increase in doublon density by the end of the pulse [see for example Fig. 2(b)]. Since we are in the tunnel ionization regime [Eq. (7)], we expect that plotting $\Gamma_{\text{tunnel}}$ against $F_0^{-1}$ on a log scale will produce a linear plot with negative slope $-\frac{\pi}{2}\frac{\Delta_{\text{Mott}}}{\xi}$. We can then estimate the value of $\xi$ from the linear fits by assuming that $\Delta_{\text{Mott}}$ does not change appreciably from its uncoupled value and deduce the effect of coupling $g$ on correlation length $\xi$.

We calculate the rate of production $\Gamma = dD(t)/dt$ by plotting the ground state doublon density [Eq. (3)] as a function of time, fitting it to a tanh function,

$$D(t) = D_0 + a\big[\tanh b(t - t_{\text{th}}) + 1\big], \tag{8}$$

and extracting the slope [14]. Figure 2(b) shows $D(t)$ as a function of time for $F_0 > F_{\text{th}}$, along with the fitting curve. The maximum production rate can be extracted as $\Gamma = ab$, the slope of the fit at the time of maximum doublon production.

Figure 3 shows log plots of $\Gamma$ versus $F_0^{-1}$ for small couplings $0.05t_0 \leq g \leq 0.2t_0$ (with increasing coupling down the panels) and $U = 5t_0$. The downward sloping graphs can be fitted with straight lines and $\xi$ extracted from the slope $m = -\frac{\pi}{2}\frac{\Delta_{\text{Mott}}}{\xi}$. We notice that as $g$ is increased, $\xi$ significantly increases even with a very small increase in coupling.

The R-squared values are also calculated for the linear fits as

$$R^2 = 1 - \frac{\sum_i (y_i - f)^2}{\sum_i (y_i - \bar{y}_i)^2}, \tag{9}$$

where $y_i$ are the $y$-values for the data points, $f$ is the value of the linear fit, and $\bar{y}$ is the average $y$-value. The values shown for most of the plots in Fig. 3 are close to one, confirming the exponential dependence of charge production on the driving field [Eq. (7)] typical of the tunnel ionization regime.

To verify our results, we conducted independent DMRG calculations which extracted $\xi$ from calculations of the single-particle Green's functions $G(|x|)$. Derived from the charge stiffness, the correlation length is related to the equal time single-particle Green's function $G(|x - x'|) = \langle 0|c_{x'}^\dagger c_x + c_x^\dagger c_{x'}|0\rangle$, which is shown to scale as

$$G(|x|) \sim \exp(-|x|/\xi). \tag{10}$$

This definition of $\xi$, derived from the Green's function, was used in density matrix renormalization group (DMRG) calculations [30] presented here.

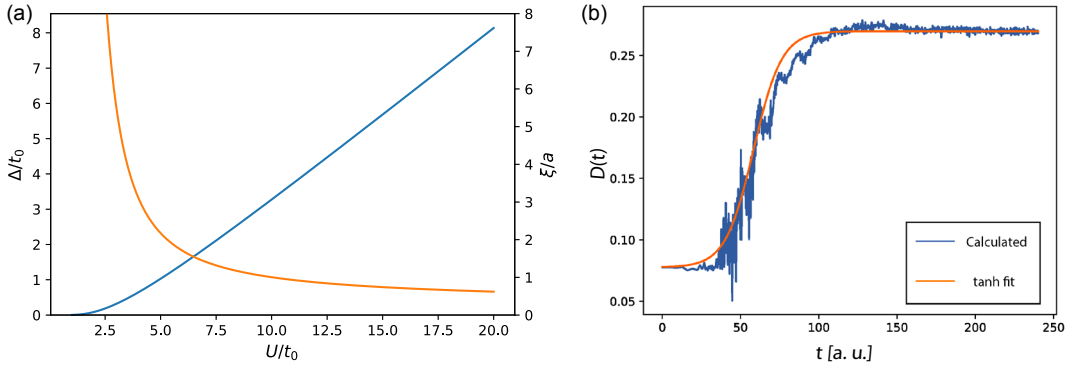


**Fig. 2.** (a) Mott gap $\Delta/t_0$ [24] (in blue) and doublon-hole correlation length $\xi/a$ [27] (in orange), as functions of Hubbard repulsion $U/t_0$. (b) Doublon density as a function of time. $D(t)$ starts at a low value and increases as the pulse ramps up and saturates at a higher value. The curve is fitted to a tanh function [Eq. (8)] to extract the slope [14].

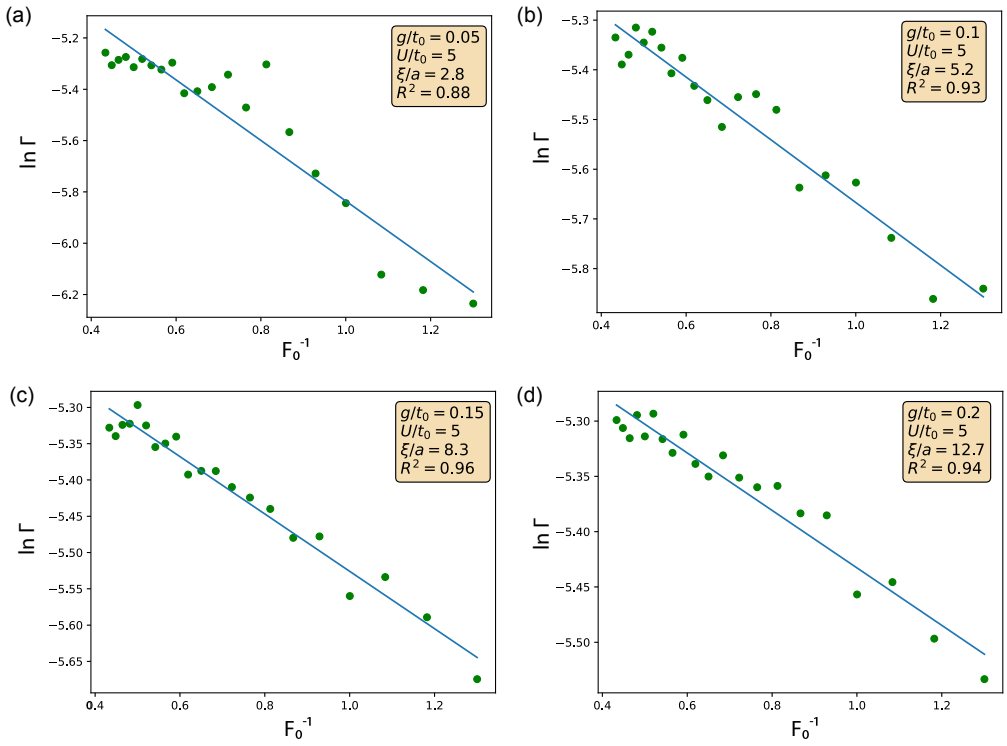


**Fig. 3.** ln Γ versus $F_0^{-1}$ plots for small couplings $0.05t_0 \leq g \leq 0.2t_0$ (with increasing coupling to the right) for two values of Hubbard $U = 4t_0$ (a)–(d) and $U = 5t_0$ (e)–(h). Notice how even a small coupling to a metal drastically increases the correlation length.

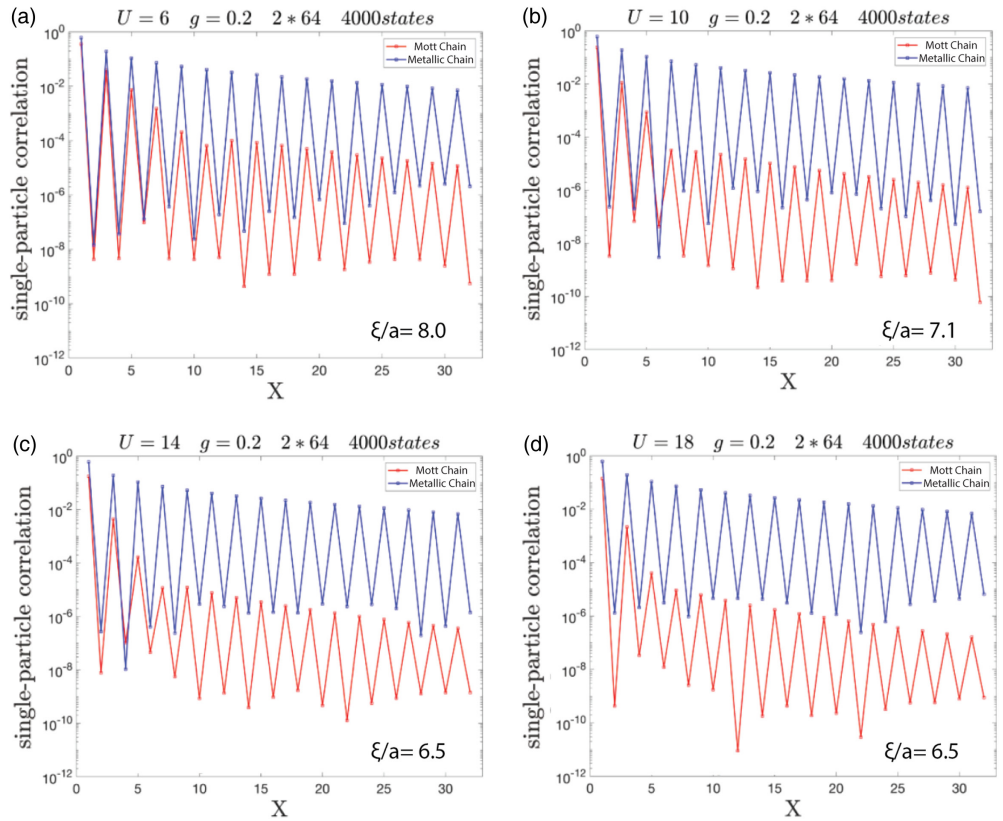


**Fig. 4.** DMRG results plotting single-particle Green's function versus lattice site for the Hubbard chain (red) and the metallic chain (blue). The interchain coupling $g = 0.2t_0$ for all plots, and the Hubbard value is given on top of each plot. The plots are semi-log, showing the exponential decay of the Green's function and indicating the gapping of the charge mode. We see the usual trend of $\xi$ decreasing with increasing $U$.

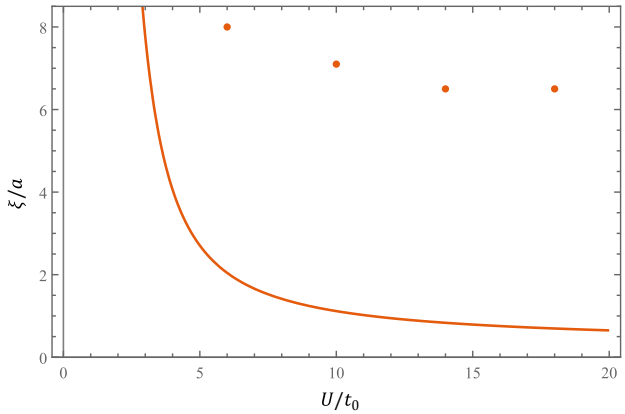


**Fig. 5.** Correlation length $\xi$ for the uncoupled ($g = 0$) insulator [27] [same as in Fig. 2(a)] and for small coupling $g = 0.2t_0$ from DMRG results.

The geometry of the model considered was extended to a $2 \times 64$ ladder with the open boundary conditions, keeping 4096 SU(2) multiplets and discarding weights smaller than $10^{-7}$. The results are shown in Fig. 4 for the value of $g = 0.2t_0$ and varying values of $U$. The plots show $G(|x|)$ for both Hubbard and free chain. The Hubbard chain, which is the focus of our results, shows a linear trend with negative slope in the long-distance behavior. This should be expected as we anticipate $G(|x|) \sim \exp\{x/\xi\}$. From the slope, we can therefore extract $\xi$. These values are displayed in the bottom-right of each plot and are plotted in Fig. 5 to be compared with $g = 0$, again showing the significant increase in $\xi$ as a result of increasing $g$. Another observation from Fig. 4 is that while the function $G(|x|)$ slopes down linearly on the whole, it also displays oscillatory behavior on the short length scale with a period equal to $2a$. This can be related to the fact that the lowest energy single-particle excitations in the model occur at $k = \frac{\pi}{2a}$ [31].

## 4. CONCLUSION

In conclusion, we proposed a method for extracting the doublon-hole correlation length from a highly nonlinear response of a Mott insulator driven by a strong laser field. We then applied this method to demonstrate that the correlation length inside the Mott insulator is significantly increased by the presence of a metallic layer, allowing for an increased mobility of carriers. The tunability of interlayer coupling, $g$, between the magnetic insulator and the metallic layer could lead to significant advances in the application of Mott insulators as memristors in a neuromorphic network [32,33]. In particular, increasing the coupling value, $g$, could model long-term potentiation, a key mechanism underlying learning in a neural network, whereby the cell has a lower threshold for a response. In our model, this would correspond to a lowered threshold in the driving electric field needed for the Mott insulator breakdown. As described above, this lower threshold is physically implemented by the increased correlation length with an increasing value of $g$. The fact that correlation length increases dramatically even for small increases in coupling suggests that this type of control is experimentally feasible and could be mediated by decreasing the distance between the metallic and insulating layers (by increasing external pressure, for instance).

Furthermore, our work can be used to extract correlation length from experimental measurements of a Mott insulator driven by strong laser fields in the tunneling regime, corresponding to a small value of the Keldysh parameter, $\gamma_K$. The relevant experimental observable has to correlate with the rate of doublon-hole production in the tunneling regime, given by Eq. (7). This can be found in high harmonic generation experiments, where it was previously shown that the rate of doublon-hole production correlates closely with the intensity of high harmonics [15,22]. Alternatively, recent experiments measuring differential reflectivity $\Delta R/R$ [23] can also be used to obtain the rate of doublon-hole production, $\Gamma$, and thereby extract the doublon-hole correlation length. The ability to extract correlation length directly from experimental data can be used to experimentally validate existing theoretical models of correlated electronic systems.

**Funding.** Division of Materials Research (DMR-2011876).

**Acknowledgment.** This work was supported by the Center for Emergent Materials, an NSF MRSEC.

**Disclosures.** The authors declare no conflicts of interest.

**Data availability.** Data underlying the results presented in this paper are not publicly available at this time but may be obtained from the authors upon reasonable request.

## REFERENCES

1. L. V. Keldysh, "Ionization in the field of a strong electromagnetic wave," Zh. Eksp. Teor. Fiz. **47**, 56–63 (1964).
2. C.-T. Liang, Y.-Y. Wu, Z.-B. Wang, *et al.*, "Evolution of the frequency-comb structure and coherence from a Keldysh multiphoton into a tunneling regime," Opt. Express **30**, 2413–2423 (2022).
3. S. Popruzhenko, "Keldysh theory of strong field ionization: history, applications, difficulties and perspectives," J. Phys. B **47**, 204001 (2014).
4. G. Orlando, C. McDonald, N. Protik, *et al.*, "Identification of the Keldysh time as a lower limit for the tunneling time," Phys. Rev. A **89**, 014102 (2014).
5. A. S. Kornev and B. A. Zon, "Keldysh theory of tunnel ionization of an atom in a few-cycle laser pulse field," Phys. Rev. A **85**, 035402 (2012).
6. N. Takamura, T. Miyamoto, S. Liang, *et al.*, "Efficient Mott insulator-metal transition by an intense terahertz electric field pulse via quantum tunneling," Phys. Rev. B **107**, 085147 (2023).
7. S. Banerjee, U. Kumar, and S.-Z. Lin, "Inverse faraday effect in Mott insulators," Phys. Rev. B **105**, L180414 (2022).
8. S. Imai, A. Ono, and S. Ishihara, "High harmonic generation in a correlated electron system," Phys. Rev. Lett. **124**, 157404 (2020).
9. K. Hejazi, J. Liu, and L. Balents, "Floquet spin and spin-orbital Hamiltonians and doublon-holon generations in periodically driven Mott insulators," Phys. Rev. B **99**, 205111 (2019).
10. C. Aron, "Dielectric breakdown of a Mott insulator," Phys. Rev. B **86**, 085127 (2012).
11. Z. Lenarčič and P. Prelovšek, "Dielectric breakdown in spin-polarized Mott insulator," Phys. Rev. Lett. **108**, 196401 (2012).
12. N. Tsuji, T. Oka, and H. Aoki, "Correlated electron systems periodically driven out of equilibrium: Floquet+ DMFT formalism," Phys. Rev. B **78**, 235124 (2008).
13. T. Oka, R. Arita, and H. Aoki, "Breakdown of a Mott insulator: a nonadiabatic tunneling mechanism," Phys. Rev. Lett. **91**, 066406 (2003).
14. T. Oka, "Nonlinear doublon production in a Mott insulator: Landau-Dykhne method applied to an integrable model," Phys. Rev. B **86**, 075148 (2012).

15. R. Silva, I. V. Blinov, A. N. Rubtsov, *et al.*, "High-harmonic spectroscopy of ultrafast many-body dynamics in strongly correlated systems," Nat. Photonics **12**, 266–270 (2018).
16. Y. Murakami, M. Eckstein, and P. Werner, "High-harmonic generation in Mott insulators," Phys. Rev. Lett. **121**, 057405 (2018).
17. Y. Murakami, S. Takayoshi, A. Koga, *et al.*, "High-harmonic generation in one-dimensional Mott insulators," Phys. Rev. B **103**, 035110 (2021).
18. K. Uchida, G. Mattoni, S. Yonezawa, *et al.*, "High-order harmonic generation and its unconventional scaling law in the Mott-insulating $Ca_2RuO_4$," Phys. Rev. Lett. **128**, 127401 (2022).
19. C. Orthodoxou, A. Zaïr, and G. H. Booth, "High harmonic generation in two-dimensional Mott insulators," npj Quantum Mater. **6**, 76 (2021).
20. M. Eckstein, T. Oka, and P. Werner, "Dielectric breakdown of Mott insulators in dynamical mean-field theory," Phys. Rev. Lett. **105**, 146404 (2010).
21. J. Li, C. Aron, G. Kotliar, *et al.*, "Electric-field-driven resistive switching in the dissipative Hubbard model," Phys. Rev. Lett. **114**, 226403 (2015).
22. A. AlShafey, G. McCaul, Y.-M. Lu, *et al.*, "Ultrafast laser-driven dynamics in metal/magnetic-insulator interfaces," Phys. Rev. B **108**, 144434 (2023).
23. X. Li, H. Ning, O. Mehio, *et al.*, "Keldysh space control of charge dynamics in a strongly driven Mott insulator," Phys. Rev. Lett. **128**, 187402 (2022).
24. F. H. Essler, H. Frahm, F. Göhmann, *et al.*, *The One-dimensional Hubbard Model* (Cambridge University, 2005).
25. T. Giamarchi, *Quantum Physics in One Dimension* (Clarendon, 2003), Vol. **121**.
26. P. Coleman, *Introduction to Many-body Physics* (Cambridge University, 2015).
27. C. Stafford and A. Millis, "Scaling theory of the Mott-Hubbard metal-insulator transition in one dimension," Phys. Rev. B **48**, 1409–1425 (1993).
28. V. Sunko, F. Mazzola, S. Kitamura, *et al.*, "Probing spin correlations using angle-resolved photoemission in a coupled metallic/Mott insulator system," Sci. Adv. **6**, eaaz0611 (2020).
29. J. Schwinger, "On gauge invariance and vacuum polarization," Phys. Rev. **82**, 664–679 (1951).
30. U. Schollwöck, "The density-matrix renormalization group," Rev. Mod. Phys. **77**, 259–315 (2005).
31. A. Abdelwahab, E. Jeckelmann, and M. Hohenadler, "Ground-state and spectral properties of an asymmetric Hubbard ladder," Phys. Rev. B **91**, 155119 (2015).
32. D. Strukov, G. S. Snideer, D. R. Stewart, *et al.*, "The missing memristor found," Nature **453**, 80–83 (2008).
33. F. Peronaci, S. Ameli, S. Takayoshi, *et al.*, "Mott memristors based on field-induced carrier avalanche multiplication," Phys. Rev. B **107**, 075154 (2023).

164.107.250.239 2025-04-01 11:29